Design of Circularly Polarized Microstrip Antenna with slotted Split ring array for Video Surveillance Applications at C-Band

Shipra Srivastava[1], Saptarshi Gupta[2], Vibhav Kumar Sachan[3], Satya Sai Srikant[4*]

[1,2,4]Department of Electronics and Communication Engineering, SRM Institute of Science and Technology, Delhi NCR Campus, Modinagar, Ghaziabad, Uttar Pradesh 201204 India; Email: satya.srikant2311@gmail.com

[1,3]Department of Electronics and Communication Engineering, KIET Group of Institutions, Delhi NCR Campus, Muradnagar, Ghaziabad, Uttar Pradesh 201206 India.

Abstracts: It has been observed that the circularly polarized antenna always play an important role in modern wireless communication applications. One of such applications is Video surveillance system. Such system interfaced with circularly polarized antenna during natural calamities, which plays a crucial and important role in rescuing the survivors. The weather conditions make it hard to achieve effective communication between the surveillance equipment and the controller. The applications of rescuing vehicle/boat movement during flood-affected areas required an uninterrupted wireless connectivity, for which polarized antennas are very much required. The present paper investigates this problem by designing an efficient circularly polarised antenna on metasurface material consisting of split ring resonator. The designed antenna is designed to operate in the frequency range of 7.1-7.23 GHz. FR4 glass epoxy material is used as an antenna substrate with dielectric constant 4 and thickness of 1.6mm. An array of split ring resonators etched microstrip antenna was fabricated on FR4 glass epoxy substrate. The result obtained with such a microwave antenna produces an excellent gain of 7.4 dB and return loss of 17.7dB with a bandwidth of 1.2 GHz. Future studies are still in progress.

Keywords: Microstrip Antenna, FR4 Epoxy Substrate, Metasurface, Circular Polarization, Video Broadcasting.

1. INTRODUCTION

Video surveillance is becoming now a days increasingly important in the fight against crime and the protection of public safety. It is also being used for a variety of other purposes, such as security monitoring, fraud detection, compliance, flood-survey during natural calamities, coal mining surveillance and many more applications [1-2]. In the older times, only static CCTV or any static devices were used for surveillance applications. Wireless communication has enabled advanced technology such as unmanned aerial vehicle (UAV's) with cameras, are now a day's widely used for various application [3]. Different surveillance cameras are shown in Fig 1 as various examples. The challenges of wireless video surveillance technology are its limited quality of the video footage because it requires large bandwidth and higher frequency to stream the high-quality video footage. Many companies started to operate the frequencies to resolve problem without any established regulations, but this lead to a different kind of problem. Different industries started to use their standards sometimes this would cause ambiguity and creates confusion between the devices. To overcome these constrains the ITU has suggested some standards to use for various industrial applications. One of them is ITU-R BT.2069-7(10/2017) which specifies that the frequencies can be used for video broadcasting [4]. This research work concentrates on the 7.1-7.3 GHz band for the surveillance application, as very few research has attempted in the range of 6.5 – 8 GHz.

Fig. 1. Video surveillance camera for (a) Static mode with wire antennas (b) Boat with dome shaped antenna (c) Flood monitoring with pyramidal shaped antenna (d) Industrial monitoring

TABLE 1
POTENTIAL TUNING RANGE FOR CONSIDERATION OF ELECTRONIC NEWS GATHERING (ENG) FOR INDIA [4]

Country	Ranges	Application
India	6.425-7.125 MHz; 7150-8700 MHz, 11.7-12.3 MHz	Microwave links for video transmission
Australia	1980-2110 MHz; 2170-2300 MHz; 2500-2690 MHz; 7100-7425 MHz; 8275-8400 MHz; 12.75-13.25 GHz, 21.2 -23.6 GHz	Mobile vehicular an airborne video links, point to-point video links, portabl video links and cordles cameras may be used in som or all of these bands
Brazil	3300-3400 MHz; 6650-7130 MHz	Point-to-point, portable vide links and cordless camera
	7130-7410 MHz; 10.15-10.30 GHz 10.50-10.65 GHz	Point-to-point audio an video streaming link between TV stations
Russian Federation	7150-8700 MHz	Cordless cameras an temporary point-to poir video links

ITU recommendations regarding microwave link for video communication range are presented in Table 1 with few countries examples. Generally, high frequency communications are affected by the weather conditions such as fog and heavy rain [5]. Many researchers has designed and fabricated the patch antenna for long distance communications and vedio surviellience applications with or without metasurfaces [6-17] but few researchers can able to design the antenna perfectly considering many parameters. For example, Researchers like Zamani and his research team[18], Karim and his teammates [19], S Kumar and A Kumar [20] designed the antenna for vedio purpose with the parameter of return loss, gain and bandwith but they have not given any information about the circular polarization of patch antenna. Continious research work still in progress to design the circular polarized antenna with better gain.

The present research work are also focuses on designing of circularly polarized antenna for video surveillance applications. A novel wide bandwidth metasurface antenna is being used for Video Surveillance Appliances with duo concepts. Firstly array of annular split ring are used to achieve wide bandwidth and minimize the return loss and secondly, the circular slot and the spacing among them are selected in such a way that, it will provide the wider bandwidth. Two types of annular split ring array based polarized antennas were designed i.e the array of (1×2) matrix and array of (3 x 5) matrix for the video survelliance applications. Metasurface beneath the main substrate is used to achieve the desire circular polarization. All the investigations were first simulated and then fabricated with FR4 epoxy substrate to obtain the beam forming and broad radiation pattern with a wider bandwidth.

2. ANTENNA DESIGN

A single element annular split ring antenna was initially designed with commercial HFSS software tools. The top view of the annular split ring antenna with dimensions is shown in Fig 2. Here FR4 glass epoxy substrate with 4.4 dielectric constant (ε_r) was used in designing the antenna, which is commercially available in two versions; one is with 0.8 mm height, and another is with 1.6 mm heightFR4 having 0.8 mm height is usually brittle in nature and it may subject to structural deformation. So, FR4 glass epoxy with 1.6 mm height was chosen as substrate it can withstand with the temperature in the range of 150° C to 200° C and also it can operate up to 10 GHz frequency. The design parameters of annular split ring antenna are shown in Table 2

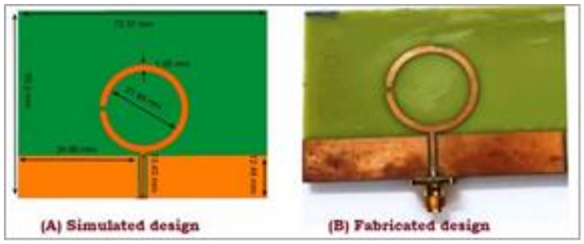

Fig 2: Top view of the annular split ring antenna (A) Simulated design (B) Fabricated design

The antennas substrate dimensions were primarily calculated using the below equations and adjusted to the requirements later. These optimized values are obtained by trial and error procedure. The final design values are tabulated in Table 2.

Width of the Patch Antenna

$$W = \frac{c}{2f_r\sqrt{\frac{(\varepsilon_r + 1)}{2}}} \quad (1)$$

where: c = speed of light = $3x10^8$ m/s; ε_r = dielectric constant = 4.4; f_r = resonant frequency

Actual Length of Patch

$$L = L_{eff} - 2\Delta L \quad (2)$$

Effective Length of the Patch Antenna

$$L_{eff} = \frac{c}{2f_r\sqrt{\varepsilon_r}} \quad (3)$$

Extension of the Length

$$\Delta L = 0.412h\frac{(\varepsilon_{eff} + 0.3)\left(\frac{W}{h} + 0.264\right)}{(\varepsilon_{eff} - 0.258)\left(\frac{W}{h} + 0.8\right)} \quad (4)$$

$$W_s = W + \lambda \quad (5)$$

$$L_s = L + \lambda \quad (6)$$

Here W_s provides the width of substrate and L_s is length of the substrate The annular split ring antenna with an array of (1 X 2) matrix was designed for the frequency 7.15 GHz to enhance overall gain. Fig 3 shows antenna array configuration.

TABLE 2 ANTENNA DESIGN PARAMETERS

Substrate Parameters	Values (mm)
Length	72.37
Width	52.2
Height	1.6
Split ring resonator (SRR) Inner Radius	21.89
Split ring resonator (SRR) Width	1.95
Ground length	34.86
Ground Width	12.48
Feed Length	13.45

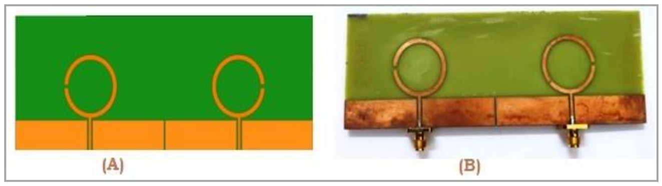

Fig 3 Antenna array with 1 x 2 configuration as a (A) Simulated design (B) Fabricated design.

The wide bandwidth was achieved with the split ring resonators (SRR), which act as resonating elements. The structures of SRR are created by the etching on FR4 epoxy substrate. The single element split ring resonators (SRR) top view with dimensions is shown in Fig 4. With repect to the desired operating frequency and gain, a metasurface was designed to achieve the desired circular polarization [16-20].

The designed metasurface consists of double split-ring structure (SRR) on FR4 epoxy substrate layer of thickness 1.6mm. The dimension and arrangements of SRR's on the metasurface are shown in Fig 5. It was observed that for achieving the circular polarization, the gap (0.8mm) in between antenna and the metasurface was optimized by trial method.

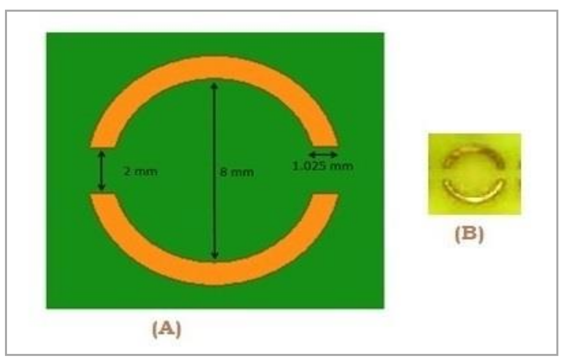

Fig 4 Metasurface single element- SRR top view and dimensions (A) Simulated design (B) Fabricated design

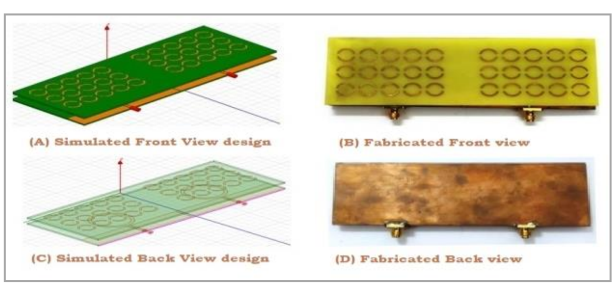

Fig 5 SRR Array arrangements on metasurface (A) Simulated Front View design (B) Fabricated Front view (C) Simulated Back View design (D) Fabricated Back view

3. RESULTS AND DISCUSSION

The prototype of the fabricated antenna and anechoic chamber (isolated room free of electromagnetic signals) measurement setup is shown in Fig 6. The return loss (S_{11}) and gain of the antenna (dB) are measured using Vector Network Analyzer (VNA).

Fig 6 Prototype antenna (A) Top view (B) Measurement setup of antenna in anechoic chamber for performance

There was no change at all in the performance for return loss of the proposed antenna (as shown in Fig 7) of with a design of (1 x 2) matrix in the presence and absence of metasurface. Both the proposed antenna showed the return loss of – 17.7 dB @ 7.2 GHz and its bandwidth showed 1.2 GHz with the centre frequency of 7.2 GHz in the range of in the range between 6.6 GHz to 7.8 GHz. The antenna gain of proposed antenna without and with metasurface are shown in Fig 8 and Fig 9 respectively. The observed gain of the proposed antenna without metasurface array is 6.38 dB where as the gain with metasurface increased to 7.44 dB. The radiation pattern of proposed antenna with metasurface as shown in Fig 10 was found that after insertion of metasurface over the antenna with a pre-decided air gap, there is an increase in the antenna gain by 1.1 dB with the same radiating pattern.

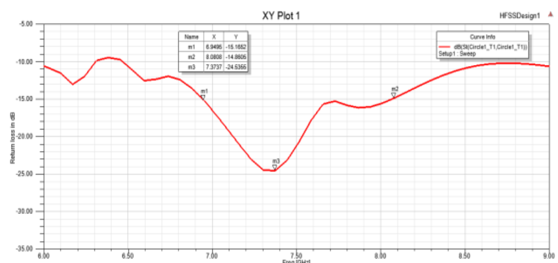

Fig 7 Return loss (dB) both with and without metasurface

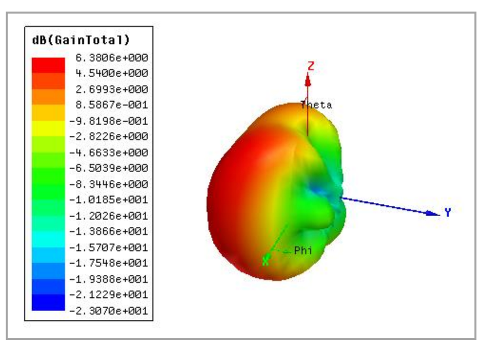

Fig 8 Gain without metasurface

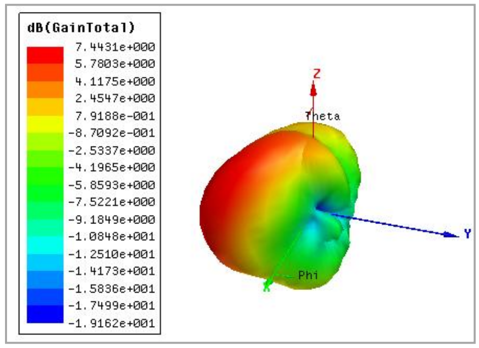

Fig 9 Gain with metasurface

Fig 10 Radiation pattern with metasurface

It has been observed that the antenna without metasurface at the required frequency band has an axial ratio of about 18.53 dB, but did not show the circular polarization (as shown in Fig 11). After the deployment of the metasurface, it has been observed that the radiation from the antenna array became circularly polarized from frequency band of 7.09 GHz to 7.23 GHz, which was evident by the axial ratio (as shown in Fig 12). When the magnitude of left-hand circular polarized (LCHP) and right-hand circular polarization (RCHP) were characterized and measured in metasurface based proposed antenna, the results showed that the most of radiation is LCHP (20.15) and there is only a tiny amount of radiation in RCHP (0.04) refer to Fig 13.

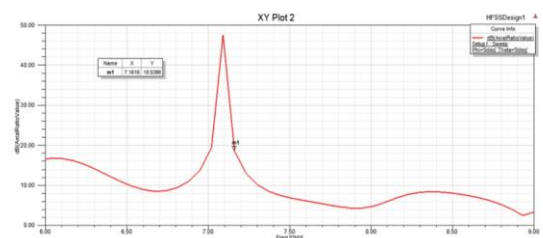

Fig 11 Axial ratio without metasurface (no circular polarization observed)

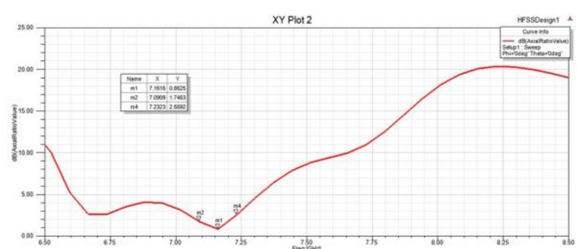

Fig 12 Axial ratio with metasurface (Circular polarization observed)

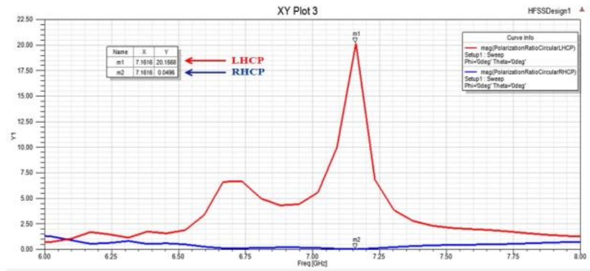

Fig 13 Plot of Left Right Hand Circular polarization (LHCP) and Right Hand Circular Polarization (RHCP) of antenna with metasurface

The gap in between antenna and the metasurface for achieving the left and right hand circular polarization is optimized using the trial and error method in simulated results which was then fabricated. The variations in the axial ratio were noted down at 7.16 GHz for every 0.2 mm step during the experiment as tabulated in Table 3. The observations were plotted for analysis refers to Fig 14. The optimum gap between the antenna array and the metasurface was observed to be 5.6 mm. Any other values would not produce circular polarization with the respective setup because the axial ratio obtained with other distance is not closer to zero. The split rings on the metasurface were the prime elements in achieving the circular polarization; the split gaps were also optimized using the trial and error procedure. The observations were tabulated in Table 4 and visualized using line graph Fig 15.

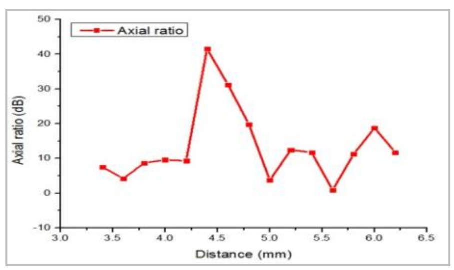

Fig 14 Plot between Axial ratio and distance

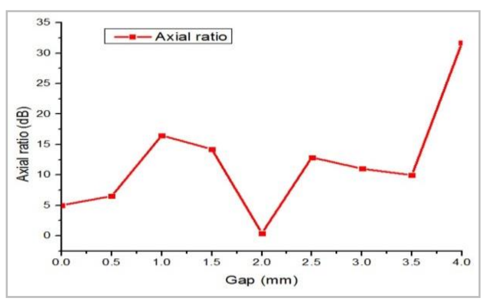

Fig 15 Plot between Axial ratio and split gap

TABLE 3 VARIATION OF AXIAL RATIO WITH DISTANCE BETWEEN ANTENNA AND METASURFACE

Distance (mm)	Axial Ratio(dB)
3.4	7.52
3.6	4.2
3.8	8.7
4	9.6
4.2	9.3
4.4	41.6
4.6	31.2
4.8	19.8

5	3.68
5.2	12.46
5.4	11.7
5.6	0.86
5.8	11.22
6	18.74
6.2	11.75

TABLE 4 AXIAL RATIO WITH SPLIT RATIO VARIATIONS

Split gap (mm)	Axial Ratio (dB)
0.0	5.0258
0.5	6.5481
1.0	16.4888
1.5	14.2505
2.0	0.4301
2.5	12.8953
3.0	11.0344
3.5	9.9812
4.0	31.7011

The antenna has two terminals with VSWR, which was well observed under acceptable level i.e. VSWR < 2. The terminal one and terminal two has VSWR of 1.19 and 1.20 respectively. All the above investigations showed that after the insertion of metasurface, the antenna performances had increased, almost in all parameters (as shown in Table 5). Table 5 provides a brief summary about the performance comparision of antenna design with and without metasurface. It was also observed that on insertion of metasurface, there was not only a change in overall bandwidth by 0.1 GHz but also the antenna gain has been increased by 1.06 dB with circular polarization in the frequency range between 7.09 GHz to 7.23 GHz; a basic requirement for video surveillance appliances at microwave range.

TABLE 5 PERFORMANCE COMPARISION OF THE PROPOSED ANTENNA WITH OR WITHOUT METASURFACE

Parameters	**Antenna Configurations**	
	Without metasurface	**With metasurface**
Operating range	6.67 GHz to7.86 GHz	6.9 GHz to 8 GHz
Return Loss	-17.7 dB at 7.2 GHz	-17.7 dB at 7.2 GHz
Gain	6.38 dB	7.44 dB
Bandwidth	1.2 GHz	1.3 GHz
Polarization	Linear polarization	**Circular polarization** (7.09 GHz to 7.23 GHz)

Table 6 also provides a brief summary about the performance comparison of proposed antenna design with existing antenna design. It is observed from Table 6 that the present research work for designing of circularly polarized mictrostrip antenna on metasurface, slotted with a matrix of double split-ring structure (SRR) on FR4 epoxy substrate layer provides excellent results for video surveillance applications in terms of gain, effective return loss, and wide bandwidth. Future studies are still in progress for reconfigurability in nature.

TABLE 6 PERFORMANCE COMPARISION OF THE PROPOSED DESIGN WITH EXISTING DESIGN

Ref. No.	Year	f_o (GHz)	Return Loss (S_{11}) dB	Gain (dB)	BW (GHz)	Polarization
[18]	2016	8.025 8.075 8	-15.76 -24.38 -17.99	5.83 5.15 6.58	0.5	No information
[19]	2019	28 28	-43.23 -67.37	7.69 7.75	0.792 0.660	No information
[20]	2021	7.25 6.80	-21 -32	9 5	0.31 1.42	No information
Present work	2023	6.9-8	-17.7	7.44	1.2	**Circular polarization** 7.09 GHz to 7.23 GHz

CONCLUSIONS

The prototype metasurface based antennas array were designed and fabricated with and without metasurface substrate, in the frequency range of 6.9 GHz-7.2GHz for video surveillance applications. The results of prototype fabricated metasurface based antenna not only provide excellent gain of 7.44 dB with acceptable return loss of -17.7 dB, but also operates with perfect circularly polarization in the frequency band of 7.23 GHz -7.9 GHz. As per available literature, till now no researchers have obtained circular polarization with such antenna characteristics, particularly in the frequency range of 6.9 – 8 GHz. The properties of circularly polarized antenna are immune to noise caused by extreme weather conditions and able to stream high-quality video. The fabricated antenna with metasurface has sufficient gain for effective communication and surveillance video applications and it also compliances with the ITU suggested technical specifications. Hence the proposed design antenna can be used with any kind of unmanned aerial vehicle (UAV) systems, which involve in video surveillance during natural calamities. Future studies are in progress for achieving the reconfigurable circularly polarized antenna with high gain.

ACKNOWLEDGEMENTS

All the authors are thankful to higher management of SRM Institute of Science and Technology, Delhi-NCR campus, Modinagar for allowing their research work related to antennas.

REFERENCES

[1] Puvvadi U L N, Benedetto K D, Patil A, Kang K, Park Y. 2015. Cost-Effective Security Support in Real-Time Video Surveillance. IEEE Trans on Ind Inf. 11(6):1457-1465.

[2] Xu Y, Xue Y, Hua G, Cheng J. 2020. An Adaptive Distributed Compressed Video Sensing Algorithm Based on Normalized Bhattacharyya Coefficient for Coal Mine Monitoring Video. IEEE Access. 8:158369-158379.

[3] Shakhatreh H, Ahmad H S, Al-Fuqaha A, Dou Z, Almaita E , Khalil I, Othman N S, Khreishah A, Guizani M. 2019. Unmanned Aerial Vehicles (UAVs): A Survey on Civil Applications and Key Research Challenges. IEEE Access. 7: 48572-48634.

[4] https://www.itu.int/dms_pub/itu-r/opb/rep/R-REP-BT.2069-7-2017-PDF-E.pdf)

[5] Li F, Chen W, Shui Y. 2020. Study on Connectivity Probability of Vanets Under Adverse Weather Conditions at 5.9 GHz. IEEE Access. 8: 547-555.

[6] Lin B, Lv L, Guo J, Liu Z, Ji X, Wu J. 2020. An Ultra-Wideband Reflective Linear-to-Circular Polarization Converter Based on Anisotropic Metasurface. IEEE Access. 8: 82732-82740.

[7] Akbari M, Farahani M, Sebak A, T. A. Denidni T A. 2017. Ka-Band Linear to Circular Polarization Converter Based on Multilayer Slab With Broadband Performance. IEEE Access. 5:17927-17937.

[8] Samsuzzaman M, Islam M T, Singh M J. 2018. A Compact Printed Monopole Antenna with Wideband Circular Polarization. IEEE Access. 6: 54713-54725.

[9] Han J, Cao X, Gao J, Wei J, Zhao Y, Li S, Zhao Z. 2018. Broadband Radar Cross Section Reduction Using Dual-Circular Polarization Diffusion Metasurface. IEEE Antennas and Wireless Propagation Letters. 17(6): 969-973.

[10] Lin B, Lv L, Guo J, Liu Z, Ji X, Wu J. 2020. An Ultra-Wideband Reflective Linear-to-Circular Polarization Converter Based on Anisotropic Metasurface. IEEE Access. 8: 82732-82740.

[11] Jam, F. A., Singh, S. K. G., Ng, B., & Aziz, N. (2016). Effects of Uncertainty Avoidance on Leadership Styles in Malaysian Culture, , International Journal of Advance Business and Economics Research, 14(8), 7029-7045.

[12] Wu Z, Li L, Li Y, Chen X. 2016. Metasurface Superstrate Antenna with Wideband Circular Polarization for Satellite Communication Application. IEEE Ant and Wir Prop Lett. 15: 374-377.

[13] Hong T, Wang S, Liu Z, Gong S. 2019. RCS Reduction and Gain Enhancement for the Circularly Polarized Array by Polarization Conversion Metasurface Coating. IEEE Ant and Wir Prop Lett.18(1) : 167-171.

[14] Chen Q, Zhang H. 2018. Dual-Patch Polarization Conversion Metasurface-Based Wideband Circular Polarization Slot Antenna. IEEE Access. 6: 74772- 74777.

[15] Zheng Q, Guo C, Ding J. 2018. Wideband Metasurface-Based Reflective Polarization Converter for Linear-to-Linear and Linear-to-Circular Polarization Conversion," IEEE Ant and Wir Prop Lett. 17 (8): 1459-1463.

[16] Wu Z, Liu H, Li L. 2019. Metasurface-Inspired Low Profile Polarization Reconfigurable Antenna with Simple DC Controlling Circuit. IEEE Access. 7: 45073-45079.

DOI: https://doi.org/10.15379/ijmst.v10i3.1795